Conformational Changes of the Insulin Receptor upon Insulin Binding and Activation As Monitored by Fluorescence Spectroscopy†

Jongsoon Lee,‡,§ Paul F. Pilch,‡ Steven E. Shoelson,‖ and Suzanne F. Scarlata*,⊥

Department of Biochemistry, Boston University, School of Medicine, Boston, Massachusetts 02118, Joslin Diabetes Center & Department of Medicine, Harvard Medical School, Boston, Massachusetts 02215, and Department of Physiology & Biophysics, State University of New York at Stony Brook, Stony Brook, New York 11794-8661

Received July 23, 1996; Revised Manuscript Received November 14, 1996⊗

ABSTRACT: We have characterized the changes in intrinsic fluorescence that the insulin receptor undergoes upon ligand binding and autophosphorylation. The binding of insulin to its receptor results in an increase in the receptor's fluorescence intensity, emission energy and anisotropy. We monitored the time course of the anisotropy change, and these data, coupled with studies monitoring the energy transfer from insulin receptor tryptophan donors to a fluorescent-labeled insulin, allowed us to conclude that the change in anisotropy is due to a conformational change in the receptor induced by hormone binding. Since insulin association is very fast, the time course also allowed us to estimate the slower rate of formation of this conformationally-altered state. The time course of receptor autophosphorylation was measured under similar conditions and was found to be similar to the ligand-induced anisotropy time course. The simultaneous use of two fluorescent-labeled insulin analogs also allowed us to assess the maximum distance between the two hormones bound to the receptor. Addition of ATP produces a large, seemingly instantaneous increase in anisotropy. Our observation that ATP binds to the insulin receptor in the presence and absence of insulin supports the idea that the conformational change produced by insulin binding increases the rate of autophosphorylation rather than increases ATP affinity. A suggested model for these changes is presented.

The structure, function, and biochemical properties of the insulin receptor have been extensively studied as documented in several recent reviews (Taylor et al., 1992; Tavaré & Siddle, 1993; Lee & Pilch, 1994). The insulin receptor subunit structure is a heterotetramer composed of two extracellular α chains, each disulfide-linked to a β chain and to each other. The extracellular region of the β chains connects to a 23-residue transmembrane region and then to the intracellular kinase domain. The binding of insulin to the extracellular region of the receptor initiates a signal transduction cascade by causing the intracellular kinase domain to autphosphorylate on tyrosine residues. This autophosphorylation results in the activation of the receptor's intrinsic tyrosine kinase toward exogenous and endogenous substrates. Functionally, the receptor can be thought of as a dimer with a high affinity for one molecule of insulin and a lower affinity for a second insulin molecule as manifested by negatively co-operative binding isotherms (De Meyts et al., 1973). When the α−α disulfide bond(s) of the receptor are chemically reduced, the receptor becomes monomeric and each monomer contains a single class of low-affinity binding sites (Böni-Schnetzler et al., 1987; Sweet et al., 1987). Thus, at physiological concentrations only one molecule of insulin is bound per holoreceptor (Pang & Shafer, 1983, 1984; Shoelson et al., 1993).

The insulin receptor belongs to a large family of receptor/tyrosine kinases, all examples of which are covalent or non-covalent dimers whose mechanism of activation by ligand can be described in terms of transmembrane allosteric regulation (Schlessinger & Ullrich, 1992). Thus, it is assumed that insulin binding to the α chains induces a conformational change that is transmitted to the extracellular region of the β subunit and then through the transmembrane region and to the kinase domain. Evidence for conformational changes in various domains of the receptor comes from several independent experimental approaches. Crosslinking studies reveal differences in subunit contacts between ligand-occupied and unoccupied receptor (Schenker & Kohanski, 1988; Waugh & Pilch, 1989). The differential binding of site-specific anti-receptor antibodies provides evidence for ligand- and substrate-dependent conformational states (Herrera & Rosen, 1986; Maddux & Goldfine, 1991; Perlman et al., 1989; Baron et al., 1990, 1992). Finally, kinase domain sulfhydryl residues are differentially reactive in basal *versus* activated insulin receptor (Clark & Konstantopoulos, 1993). These studies, however, describe only static differences between initial and final conformational states of the receptor.

Individual domains of the receptor have been studied in real time by fluorescence and by NMR. Insulin-dependent structural changes in the ectodomain of the insulin receptor have been documented (Schaefer et al., 1992). Conformational changes in a cytosolic kinase fragment induced by tyrosine phosphorylation have also been observed (Levine

† These studies were supported in part by grants DK36424 (to P.F.P.), DK43123 (to S.E.S.), and GM53132 (to S.F.S) from the National Institutes of Health and by Grant 93-301 from the American Heart Association (to S.F.S). J.L. was supported by a Mentor-Based Postdoctoral Fellowship from the American Diabetes Association.

* Corresponding author. Tel: (516) 444-3071. FAX: (516) 444-3432. E-mail: suzanne@physiology.pnb.sunysb.edu.

‡ Boston University, School of Medicine.

§ Current address: Joslin Diabetes Center & Department of Medicine, Harvard Medical School, Boston, MA 02115.

‖ Harvard Medical School.

⊥ State University of New York at Stony Brook.

⊗ Abstract published in *Advance ACS Abstracts,* February 15, 1997.

S0006-2960(96)01815-6 CCC: $14.00 © 1997 American Chemical Society

et al., 1991). These studies have benefited from technology that allows the expression of soluble receptor domains in large amounts, but they suffer from the fact that the characteristics of insulin binding to the receptor's ectodomain and autophosphorylation of the soluble kinase domain fragment are different from these events as they occur in the native holoreceptor. Insulin binding isotherms to the soluble ectodomain reveal linear and low-affinity binding (Schaefer et al., 1991) as compared to the high-affinity curvilinear plots seen for the native receptor. The kinetic properties of the soluble kinase domain fragment are those of the basal state for the holoreceptor (Kohanski, 1993).

Here, we present a fluorescence characterization of the conformational states of a recombinant preparation of purified insulin holoreceptor where insulin binding and ligand-induced autophosphorylation are normal. Our studies were performed by monitoring changes in the receptor's intrinsic fluorescence upon insulin binding and autophosphorylation, the latter being assessed biochemically. We have also followed changes in the properties of fluorescent-labeled insulins upon their binding to receptor. Our results show that fluorescence is a useful technique to monitor the real time changes in insulin receptor conformation and can be used to answer specific questions about the mechanism of insulin action with regard to receptor autophosphorylation and activation.

MATERIALS AND METHODS

Preparation and Purification of Protein. The insulin receptor was purified from 3T3-NIH cells which were transfected with human insulin receptor cDNA (generously provided by Drs. Takashi Kadowaki and Simeon Taylor, NIH, Bethesda, MD). To fully preserve the tyrosine kinase activity of the insulin receptor, we employed conventional chromatographic means to purify the receptor to homogeneity (O'Hare & Pilch, 1988; Hing et al., 1993). Plasma membranes were treated for 1 h in a buffer containing 2% Triton, 0.02% NaN_3, and 30 mM HEPES,[1] pH 7.6 (Lee et al., 1993). Solubilized receptor was collected from the supernatant following centrifugation at 100000*g* for 60 min, and receptor was loaded onto a Sephacryl S-400 column pre-equilibrated with 150 mM NaCl in HEPES buffer (pH 7.6) containing azide (0.02%) and Triton X-100 (0.1%) (HTA). The column fractions containing insulin binding activity were pooled and incubated with wheat germ agglutinin (WGA)-agarose overnight. After extensive washes with HTA, bound proteins were eluted from WGA-agarose with 0.3 M *N*-acetylglucosamine in 20 mM Tris (pH 7.4) and 0.1% Triton X-100. The insulin receptor was purified to homogeneity by a Mono Q column and an FPLC system (Pharmacia) using a linear gradient from 0 to 0.5 M NaCl. Concentrating the receptor and exchanging the detergent were performed by binding to a small (0.3 mL) DEAE-triacryl or Q Sepharose column. Bound receptor was washed with 10 column volumes of 30 mM HEPES, pH 7.4) and 20 mM β-octyl glucoside and eluted with 0.5 M NaCl and 10% glycerol in the same buffer. Purified receptor was aliquoted and stored at −80 °C until use. The tyrosine kinase activity of each batch of purified receptor was assessed by receptor autophosphorylation as described (Lee et al., 1993). The purity of the receptor was greater than 80% as determined by silver staining and insulin-dependent autophosphorylation was always 8−10-fold greater than basal. Typically, fifteen 400 cm^2 dishes yield 300−450 μg of pure receptor. Qualitatively similar results were observed with 4 independent receptor preparations. The actual concentration of receptor in the cuvette used for the anisotropy experiments is likely to be lower than the nominal figure since at concentrations in the vicinity of 140 nM receptor (ca. 50 μg/mL, Figure 2), we expect there may be losses due to non-specific adsorption on glass and plastic surfaces.

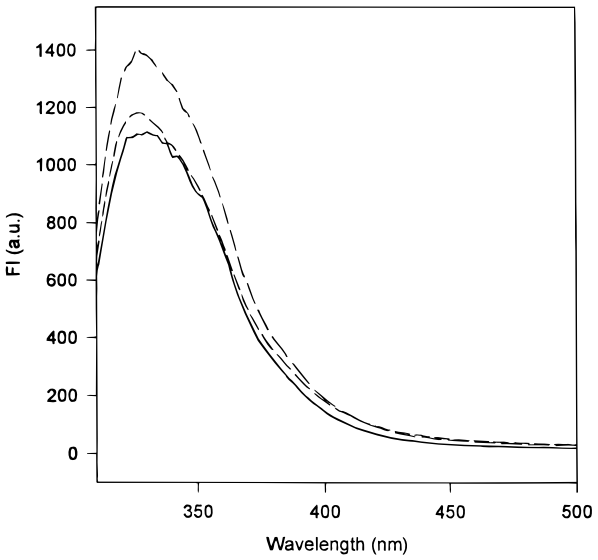

FIGURE 1: Emission spectra of the insulin receptor. Emission spectra of the insulin receptor at 0.16 μM (λ_{ex} = 295nm) in the absence of ligands (—), with 500 μM insulin (— —) and with 500 uM insulin after activation with ATP (- - -).

Autophosphorylation of the Insulin Receptor. The insulin receptor was incubated overnight with 10^{-7} M BBpa-insulin and then cross-linked under UV light with a >340 nm cutoff filter as described previously (Lee *et al.* 1993). Autophosphorylation of the receptor was performed in the presence of 50 μM ATP, 10 mM $MgCl_2$ and 8 mM $MnCl_2$. After the indicated time, the reaction was stopped by adding EDTA to the final concentration of 67 mM. Receptor was then reduced with dithiothreitol (Böni-Schnetzler et al., 1987; Lee et al., 1993) or not prior to immunoprecipitation.

Anti-Phosphotyrosine Antibody Precipitation and Western Blotting. The phosphorylated receptor was incubated with 1−2 μg of anti phosphotyrosine antibody (4G10, UBI) for 2 h at room temperature or overnight at 4 °C in the presence of 1 mg/mL of fatty acid free bovine serum albumin. The insulin receptor−antibody complex was then incubated with Protein A-Trisacryl (Pierce) for 2 h at room temperature and precipitated by centrifugation. After the supernatant was removed, the pellet was washed with HTA and was resuspended to the original volume with sample buffer (Laemmli, 1970). After 30 min at room temperature and boiling for 5 min, the receptors from the supernatant and pellet were analyzed by SDS-PAGE (Laemmli, 1970) followed by transfer onto Immobilon-P PVDF membranes

[1] Abbreviations: AMP-PNP, adenylimidodiphosphate; BBpa-insulin, benzoylphenylalanine^{B25}, B29$^{\epsilon}$-biotin insulin; EDANS-insulin, D-Gln^{A1}-[γ-5-(2-aminoethylamino)-1-naphthalenesulfonic acid] insulin; DAB-CYL-insulin, N^{ϵ}-Lys^{B29}-4-dimethylaminoazobenzene-4′-sulfonyl insulin; HEPES, *N*-(2-hydroxyethyl)piperazine-*N*′-ethanesulfonic acid; ins, insulin; IR, insulin receptor; PEG, polyethylene glycol; WGA, wheat germ agglutinin; ectodomain, the extracellular portion of the receptor; holoreceptor, the entire receptor.

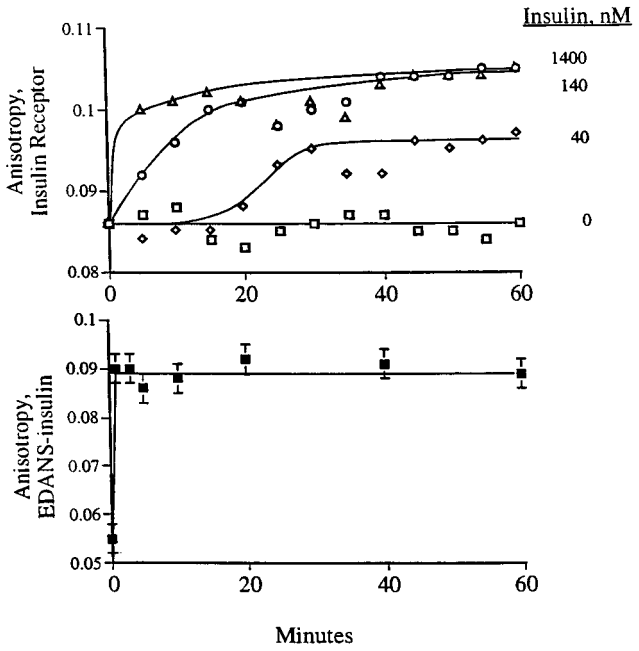

FIGURE 2: Time dependence of insulin-induced anisotropy changes in the insulin receptor and in EDANS-insulin upon ligand−receptor complex formation. (top panel) The time course for the change in anisotropy (λ_{ex} = 280 nm) of the insulin receptor at 140 nM was measured with no insulin (squares), 40 nM insulin (diamonds), 140 nM insulin (circles), and 1400 nM insulin (triangles). (bottom panel) The time course of anisotropy change in EDANS-insulin was measured upon addition of this ligand (196 nM) to receptor (96 nM). Both panels are representaive experiments (n = 4−6) with uniform errors of +0.003 as indicated in the lower panel.

(Millipore) by the method of Towbin et al. (1979). The receptor was visualized by [^{125}I]Protein A (Amersham) followed by autoradiography.

Insulin Analogs. BBpa-insulin was prepared as described in Shoelson et al. (1993). The synthesis of the fluorescent insulin analogs (EDANS- and DABCYL-insulins, and doubly modified insulin) will be described elsewhere.[2]

Spectroscopic Studies. Measurements were taken at room temperature on an ISS K-2 spectrofluorimeter (ISS, Inc., Champaign, IL) equipped with Glan-Thompson polarizers. For each measurement, 100 μl of sample in a 0.3 cm path length cuvette was used. Sample absorption was always below 0.15 OD units at the exciting wavelength. To eliminate the contribution of scattered light, 310 nm cuton filters were placed before the emission monochromater. Background signals from the buffer were never more than 1%, and no corrections to the spectra were made for this value. Anisotropy data were taken using an excitation wavelength of either 280 nm or 295 nm (as specified in the text) and an emission wavelength of 340 nm. Every reported point is an average of 6−10 measurements each with a standard deviation of ±0.001 with respect to instrument behavior. The results presented are for four different insulin receptor preparations. Each preparation gave identical spectral characteristics but differed slightly in their tryptophan anisotropy values and the extent of change with insulin binding and kinase activation. We attribute these differences to slight variations in the detergent and buffer composition, degradation products, and other environmental influences, and we do not deem them important.

[2] S.E.S., manuscript in preparation.

Table 1. Intrinsic Fluorescence Properties of IR with Ligands and KI[a]

species	intensity	n	CSM (cm^{-1})
IR	1.0	3	28 361
IR-insulin	1.35 ± 0.17	7	28 466
IR-insulin + ATP	1.09 ± 0.10	2	28 480
IR + 0.3 M KI	0.72 ± 0.12	2	28 588
IR-insulin + 0.3 M KI	0.83 ± 0.11	2	28 637
IR-insulin + ATP + 0.3 M KI	0.78 ± 0.12	2	28 686

[a] Where λ_{exc} = 295 nm and n is the number of samples and CSM is the center of spectral mass (see Materials and Methods).

The emission energies reported here refer to the center of spectral mass (CSM) in wavenumbers (cm^{-1}) which is the weighted average of the emission energy (EE) by the intensity (I) and takes into account changes in the skewness of the peak:

$$\mathrm{CSM} = (\Sigma_i \mathrm{EE}_i I_i)/(_i I_i)$$

The absorption coefficients of the IR, EDANS-insulin, and DABCYL-insulin were found to be 110 520 (λ_{exc} = 280 nm), 5249 (λ_{exc} = 340 nm), and 10 400 (λ_{exc} = 480 nm), respectively.

RESULTS

Changes in the Fluorescence Emission spectrum of the Insulin Receptor upon Ligand Binding and Autophosphorylation. We began this study characterizing the changes in the emission spectrum of the receptor when it binds insulin and ATP. The emission of the purified IR showed a strong tyrosine contribution with no evidence of contamination. The addition insulin to the receptor under conditions where both insulin binding sites are occupied results in a shift in the center of mass of the Trp toward higher energies after correcting for the small contribution of insulin (insulin contains one tyrosine and no tryptophan residues). This shift is generally correlated with a shift in the fluorophore population to less solvent-exposed environments. The emission intensity showed an initial increase with insulin binding which decreased from 5% to 15% with time up to 60 min (the longest point taken). It is unclear, however, whether the decrease was due to conformational relaxation of the protein, or to experiments factors such as absorption of the protein to the walls of the cuvette, photobleaching, or settling of the IR−insulin complex. We note that the extent of the decrease varied in the four different protein preparations and that it was unaffected by purging the sample chamber with nitrogen or agitating the sample.

To better characterize the change in solvent exposure of Trp residues with insulin binding, we titrated the collisional quencher I^- into the protein solution and monitored the extent of fluorescence quenching. We found that close to 30% of the fluorescence can be extinguished by the addition of 0.3 M KI (Table 1). The center of mass of the spectrum shifted 250 cm^{-1} to higher energies in the first 0.1 M KI and then remained constant. This shift is consistent with the quenching of solvent-exposed residues. The addition of insulin somewhat reverses quenching and further decreases the center of mass by ~50 cm^{-1}. Correlating these changes to those observed in the absence of quencher support the idea that the binding of insulin results in a decrease of exposed Trp residues.

In the absence of quencher, the addition of ATP resulted in a further shift in the Trp emission toward higher energies and a slight decrease in intensity. This decrease may be due to the introduction of charged species that can quench fluorescence into the protein matrix, as well as conformational changes associated with autophosphorylation/kinase activation. In the presence of quencher, the addition of ATP reduced the intensity (Table 1) and also shifted the emission to higher energies by a small amount, ~50 cm^{-1}. These changes with ATP addition appear to correlate with a conformational change of the protein.

Changes in Fluorescence Anisotropy of the Insulin Receptor upon Insulin Binding and Kinase Activation. To further investigate the nature of the changes seen in the emission spectrum of the receptor, fluorescence anisotropy studies were done. Fluorescence anisotropy is a measure of the rotational motion a probe undergoes during its fluorescent lifetime. In the absence of differences in lifetime, a fluorophore that is buried in a protein is generally more rotationally restricted and displays a higher anisotropy than a fluorophore free in solvent. We monitored the change in the steady state fluorescence anisotropy of the tryptophan residues of the insulin receptor and found that the anisotropy undergoes a significant increase upon insulin binding. The increase in anisotropy can be interpreted as being due to a reduction of the average rotational motion of the tryptophans. A reduction in rotational motion is in accord with the idea that insulin binding results in the burying of Trp residues. The extent of this increase and its time dependence (see below) was identical for all four IR preparations.

In Figure 2, top panel, we show the time dependence of the anisotropy change in the receptor after the addition of insulin. Control samples that did not contain insulin showed a constant anisotropy over time. These data were taken exciting at 280 nm, but similar results were observed exciting at 295 nm (data not shown). Also, identical time courses are obtained when only half the concentration of IR is used. From the data presented in Figure 2, it appears that the time course of the anisotropy increase depends on the amount of insulin added. At substoichiometric concentrations of hormone, there was a 15 min lag before a change in anisotropy was observed. A lag time is a general characteristic of overdamped, second-order systems that are usually the result of coupled first-order processes (Stephanopoulos, 1984). The scheme in footnote 3, which includes a conformational change of IR is one possibility. In this scheme, the dynamic response of the conformational change will show an overdamped, second-order dependence on the concentration of insulin added. The lag time will be very short at higher insulin concentrations and longer at lower insulin concentrations.

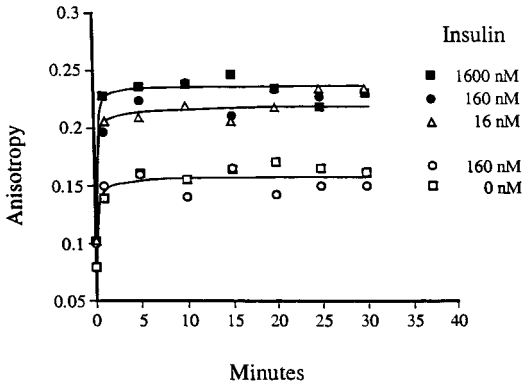

FIGURE 3: Anisotropy change of the insulin receptor by ATP. 160 nM of the insulin receptor was preincubated for 45 min at room temperature with varying amounts of insulin. Then, time course for the change in anisotropy ($\lambda_{ex} = 280$ nm) of the insulin receptor was measured after the addition of 50 μM ATP, 10 mM $MgCl_2$, and 8 mM $MnCl_2$. Data shown are for no insulin (open squares); 16 nM insulin (triangles); 160 nM insulin (filled circles); and 1600 nM insulin (filled squares). Also shown is the time course for IR + 160 nM insulin after the addition of non-hydrolyzable ATP (AMP−PNP) (open circles).

In the bottom panel, we show the change in anisotropy for EDANS-insulin at a 2:1 ligand to receptor ratio is essentially instantaneous and precedes the anisotropy change for the receptor (top panel). The result that equimolar concentrations of insulin and its receptor or a 10-fold excess of insulin over receptor induce the same degree of conformational change in the receptor suggests that only one ligand is necessary to produce the activated state, since this is the maximum possible at equimolar ligand and receptor concentrations. This is consistent with the fact that the covalent photocoupling of one insulin molecule to the receptor gives full autophosphorylation (Lee et al., 1993; see also Figure 4).

The addition of ATP to the insulin−insulin receptor complex also resulted in an increase in anisotropy (Figure 3). This occurs very rapidly and results, in part, from ATP binding since it also occurs using a non-hydrolyzable ATP analog (AMP−PNP), and it does not occur when either ATP or metals are left out of the activation buffer. Addition of ATP in the absence of metals results in only a small change in anisotropy, and preincubating the protein with ATP and measuring the time course after the addition of metals gives the identical time course obtained by adding an ATP−metal solution (data not shown). These data imply that the binding of ATP causes an initial and very rapid conformational change in the receptor. The presence of insulin markedly enhances the ATP-induced anisotropy change, presumably by allowing a second mole of ATP to bind (see Figure 5 and Discussion). It is not clear why, in the presence of 160

---

[3] The rate of conformational change in the insulin receptor due to insulin was analyzed by the following scheme:

$$\mathrm{IR} + \mathrm{ins} \underset{k_{1r}}{\overset{k_{1f}}{\rightleftharpoons}} \mathrm{IR{-}ins} \underset{k_{2r}}{\overset{k_{2f}}{\rightleftharpoons}} \mathrm{IR^*{-}ins}$$

The rate of appearance of (IR*−ins) is

$$\mathrm{d[IR^*{-}ins]}/\mathrm{d}t = k_{2f}[\mathrm{IR{-}ins}] - k_{2r}[\mathrm{IR^*{-}ins}]$$

Since $K_1 = k_{1f}/k_{2r} \approx 10^9$/M at high insulin concentration of insulins, i.e., 140 1400 nM,

$$[\mathrm{IR{-}ins}] \approx [\mathrm{IR}]_0, \text{ where } [\mathrm{IR}]_0 \text{ is the initial amount of IR}$$

$$\text{but } [\mathrm{IR{-}ins}] = [\mathrm{IR}]_0 - [\mathrm{IR^*{-}ins}]$$

$$\mathrm{d[IR^*{-}ins]}/\mathrm{d}t = k_{2f}\{[\mathrm{IR}]_0 - [\mathrm{IR^*{-}ins}]\} - k_{2r}[\mathrm{IR^*{-}ins}]$$

$$= k_{2f}[\mathrm{IR}]_0 - [\mathrm{IR^*{-}ins}](k_{2f} + k_{2r})$$

Since at $t = 0$, $[\mathrm{IR^*{-}ins}] = 0$,

$$[\mathrm{IR^*{-}ins}] = \frac{k_{2f}[\mathrm{IR}]_0}{k_{2f} + k_{2r}}(1 - \mathrm{e}^{-(k_{2f} + k_{2r})t})$$

Assuming K_2 is large (~10^2 or greater), $k_{2f} \gg k_{2r}$ and

$$[\mathrm{IR^*{-}ins}] = [\mathrm{IR}]_0(1 - \mathrm{e}^{-k_{2f}t})$$

Fitting the data for 140 and 1400 nM insulin in Figure 2, which appear to be within experimental error of each other, gives $k_{2f} = 0.16$/min = 0.0027/s.

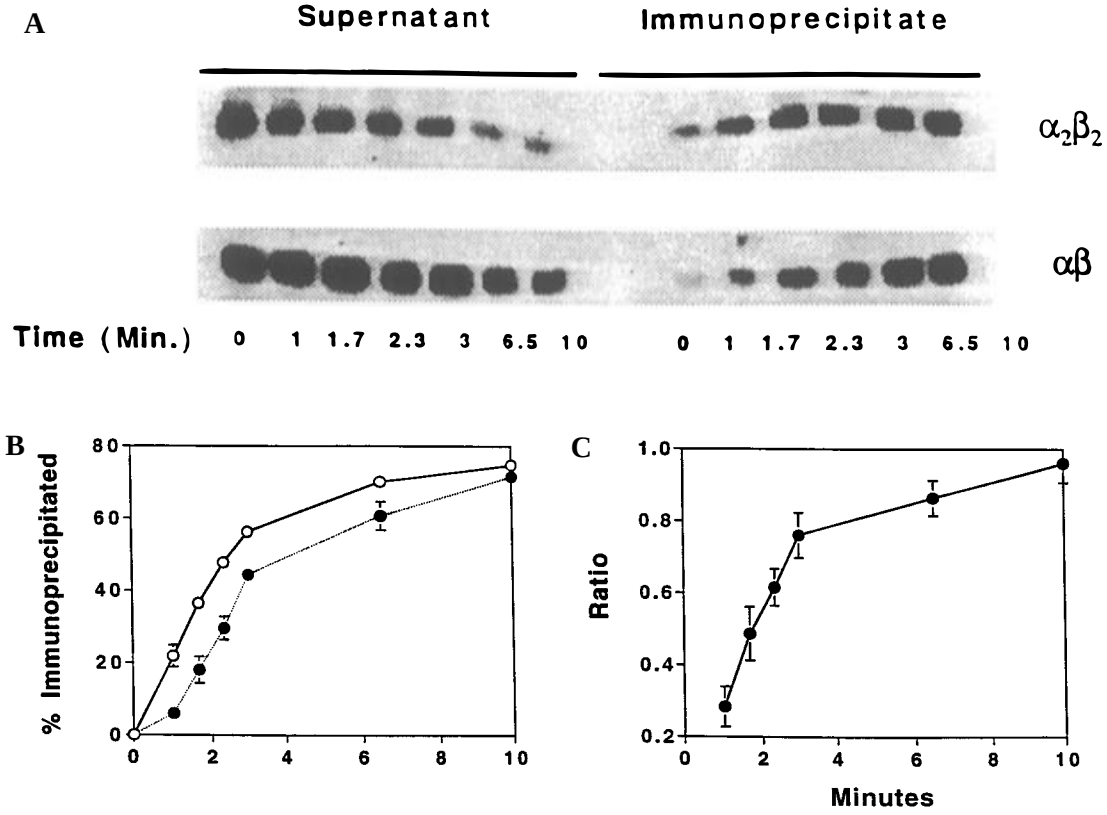

FIGURE 4: Time course of insulin receptor autophosphorylation. The insulin receptor was cross-linked with 10^{-7} M BBpa-insulin, phosphorylated with 50 μM cold ATP for the indicated times, reduced or not, and immunoprecipitated by anti-phosphotyrosine antibody as described under Materials and Methods. Protein from the supernatant and the pellet was separated in a 3−10% acrylamide gradient gel and transferred on PVDF membrane. Total insulin receptor was detected by anti-insulin receptor antibody blot using [^{125}I]Protein A (A) and was visualized by autoradiography. Quantitative analysis (by γ counter) of the immunoprecipitate is shown in panels B and C. The solid line (open circle) in panel B is for the holoreceptor, the dotted line (closed circle) for the $\alpha\beta$ half-receptor, and panel C is the ratio of the two. The results are the average + standard error of three to four determinations.

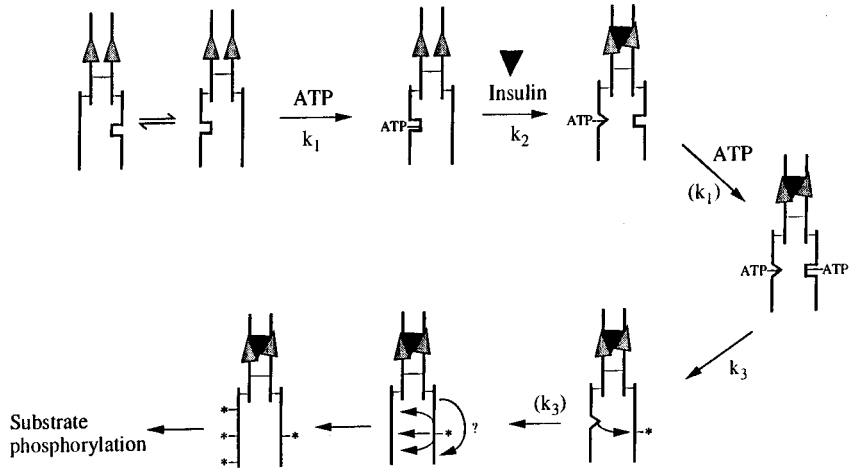

FIGURE 5: Model for the insulin receptor activation (see text).

nM insulin, hydrolyzable ATP appears to induce a greater change than AMP−PNP. Several possibilities are given in the Discussion.

Biochemical Characterization of the Time Course of Insulin Receptor Autophosphorylation. To correlate the ligand-induced conformational change observed in Figure 2 with receptor autophosphorylation and kinase activation, we examined the kinetics of this process using BBpa-insulin-linked receptor (Shoelson et al., 1993). The use of this reagent enables us to perform autophosphorylation under conditions where the receptor−ligand complex pre-exists in a non-dynamic state. Thus, the time to reach binding equilibrium between ligand and receptor need not be considered. The autophosphorylation was monitored by immunoprecipitating receptor with anti-phosphotyrosine antibody and receptor was detected in the supernatant and in the precipitate by anti-receptor antibody. Control experiments using ^{32}P-labeled receptor demonstrated the 100% efficiency of immuno-precipitation in this protocol (data not shown). As shown in Figure 4, panels A and B, the amount of the insulin receptor immunoprecipitible with anti-phosphotyrosine antibody rapidly increases with the time of autophosphorylation. Most ($\geq$70−80%) of the receptor is autophosphorylated in 6−10 min. Within a population,

receptor autophosphorylation is a stochastic process, some receptor not being phosphorylated at these times, but eventually all receptor becomes phosphorylated. This conclusion is consistent with previously published data where receptor−ligand dynamics were not controlled (Nemenoff et al., 1984). The time course of autophosphorylation is comparable to that of the insulin-dependent anisotropy change shown in Figure 2.

An additional point from this figure derives from the quantitative analysis of receptor immunoprecipitation before and after dithiothreitol treatment (panels B and C). At early times of insulin receptor autophosphorylation, we detect asymmetric receptor phosphorylation as exemplified by phosphate incorporation into only one $\alpha\beta$ half-receptor. Precipitation of 50% of the $\alpha\beta$ half-receptor at early times indicates that the initial phosphorylation event involves only one half of the receptor. In the first 2−3 min of autophosphorylation, the ratio of precipitated $\alpha\beta$ half-receptors to holoreceptor is 50% or less (see Discussion) (Figure 4C) and does not approach 100% until about 10 min. Thus, the initial autophosphorylation step occurs on only one half of the receptor, probably as a result of "*trans*" phosphorylation (see Discussion).

Studies Using Labeled Insulins. To complement the intrinsic fluorescence studies, we followed the binding of insulin labeled with EDANS at the A1 position. Labeling of the insulin did not affect its binding affinity for the receptor or receptor activation (S. E. Shoelson, unpublished results). The association of EDANS-insulin to the receptor at a 2-fold excess of ligand increases the anisotropy 0.090 ± 0.003 at $\lambda_{ex} = 360$ nm and increases the quantum yield approximately 3-fold. The emission energy also increased from 20 090 to 20 210 cm^{-1} upon IR binding indicating a shift to a less polar environment. However, this latter value is lower than the value obtained for the probe in ethanol (20 700 cm^{-1}), indicating that a substantial population of the fluorophores retains their contact with the aqueous solvent. All of the emission changes occur within the time of mixing and are constant over a period of 60 min (see Figure 2, bottom panel).

When excited, the tryptophan residues of the insulin receptor can donate their energy to the EDANS moiety. Fluorescence energy transfer depends on the distance between the probes (R) and follows an R^6 dependency. For the receptor−EDANS-insulin complex, we estimate the distance at which 50% transfer occurs to be ∼22 Å, in accord with Wang et al. (1988). Upon binding of ligand, we find that the enhancement of acceptor fluorescence exciting at 280 nm relative to 340 nm, is approximately 2-fold higher than control samples, indicating that transfer is occurring with high efficiency. Like the increase in anisotropy, energy transfer from the nearby Trp donors occurs during the time of mixing. This indicates that the conformational changes seen by intrinsic fluorescence (Figure 2) are at least partially due to residues removed form the ligand binding site. When ATP and metals are added to insulin receptor pre-incubated with EDANS-insulin, the transfer efficiency drops by a small amount but the anisotropy remains high. We interpret this change as being due to a large-scale conformational change of the protein upon kinase activation and not to dissociation of insulin from the activated receptor.

The labeled insulins will also allow us to estimate the proximity of the two insulins under conditions (high concentrations) where both are bound to the receptor. This can be accomplished by monitoring the energy transfer from A1-EDANS-insulin to B29−DABCYL-insulin. For this probe pair, the distance where the probability of transfer is 50% is 33 Å (Matayoshi et al., 1990). DABCYL is not fluorescent, and energy transfer is viewed as a loss in EDANS fluorescence due to absorption by the DABCYL group. A doubly-labeled insulin, A1-EDANS-B29-DABCYL-insulin, allowed us to calibrate the extent of transfer. Energy transfer was estimated by assuming random orientation of the probes, a refractive index equal to water, a EDANS quantum yield of yield of 0.12, and using the absorption values listed in the Materials and Methods section.

Table 2. Relative Quantum Yields of Labeled Insulins[a]

labeled insulin	buffer	+IR
EDANS-insulin	0.31 ± 0.03	0.525 ± 0.015
DABCYL-insulin	0.69 ± 0.03	0.475 ± 0.015
EDANS-insulin + DABCYL-insulin	1.05 ± 0.03	0.708 ± 0.005

[a] Data were obtained by scanning the emission spectra of the samples from 380 to 600 nm and calculating the area under the curves. The buffer is an average of three samples, while the IR is an average of five samples. The typical concentration of IR was 180 nM, and the amount of insulin was always 2-fold that concentration.

We added equimolar and different stoichiometric amounts of the two labeled insulins to the receptor under conditions where the two binding sites should be completely occupied and compared the fluorescence emission to their individual values. The results, shown in Table 2, are that half of the EDANS fluorescence is extinguished when the two are added to the receptor. Since about half of the IR is expected to have both types of insulin bound (Schäffer, 1994), this amount of energy transfer corresponds to complete transfer then between the probes. Thus, the probes are expected to have a maximum separation of ∼20 Å.

DISCUSSION

In this study we have shown that the dynamic changes involved in the activation of the insulin receptor can be followed in real time by fluorescence spectroscopy. The insulin receptor contains a large number of tryptophan and tyrosine residues that contribute to the emission (Ullrich et al., 1985; Ebina et al., 1985). When viewing only the tryptophan residues, we observe both an increase in anisotropy, a shift in the emission toward higher energies and an increase in intensity with insulin binding. All of these changes are consistent with a burial of tryptophan residues. Many regions of the α chains appear to be involved in hormone binding [see Table I in Lee and Pilch (1994)] which makes it impossible to ascribe the observed changes to particular Trp residues. It is unlikely that the observed changes in emission are due to a few residues near the insulin binding site since their contribution to the total emission of the protein is expected to be low. Rather, it is likely that the emission changes reflect overall structural changes of the holoreceptor.

Another interpretation of the emission changes of IR caused by insulin is that insulin binding alters the aggregation state of the receptor. Several lines of evidence argue against this interpretation. Characterization of IR by ultracentrifugation, gel filtration chromatography, and EM (Böni-Schnetzler et al., 1986; Morrison et al., 1988; Christainsen et al.,

1991) indicate that IR is monomeric and remains monomeric in the presence of insulin and ATP. CryoEM studies of the receptor prepared identically and subjected to the same conditions as those used here (Soon and Pilch, unpublished observations) also indicate that IR remains monomeric with insulin and ATP. It is worth noting that reducing the concentration of receptor, which might perturb the possible IR self-association, did not alter the time course of the anisotropy change of IR.

It is important to note that the purity of the IR preparations studied here varied somewhat but were always ≥80% pure. While it is conceivable that the fluorescence changes were not due to conformational changes of IR but to some contaminant in the preparation, we do not believe that this is the case since it is unlikely that an impurity would show the appropriate specific biochemical responses to these ligands. It is also unlikely that the different preparations would show identical spectroscopic changes even though the purity varied.

While there has not been a previous fluorescence study of the holoreceptor, changes in the fluorescence of the ectodomain have been characterized (Schaefer et al., 1992). Hormone binding to insulin receptor was shown to cause little change in the fluorescence intensity or emission energy but produced a significant increase in anisotropy. However, as noted in the introduction, the ectodomain has somewhat different insulin binding properties than the holoreceptor (Markussen et al., 1991; Schaefer et al., 1992). Comparison of these ectodomain results with our holoreceptor results leads to the hypothesis that a significant portion of the anisotropy increase we observe with hormone binding is caused by residues in the ectodomain whereas the changes in emission intensity an energy appear to be due to a burial of Trp residues that may be occurring in regions outside of the ectodomain. This interpretation correlates well with the idea that conformational changes associated with insulin binding need to be transmitted throughout the domains of the holoreceptor to result in transmembrane kinase activation.

Monitoring the increase in fluorescence anisotropy at varying insulin levels indicates that the time course of the anisotropy change depends on the insulin concentration at ratios of ligand to receptor of one or lower. Since we have argued that the change in anisotropy due to insulin binding is associated with a conformational change in the protein rather than a direct perturbation of a few residues in the binding pocket, then the rate for this conformational change depends directly on the concentration of the insulin-insulin receptor complex. If we assume that the binding of insulin is diffusion controlled (Figure 2, bottom panel) and, at 1400 nM insulin, that the amount of unbound receptor is zero, we can then fit the time courses in Figure 2 and roughly estimate the rate of formation of the conformationally-altered state (see footnote 3). This rate is found to be 0.0027 s^{-1} and correlates with slower backbone motions of proteins (Careri et al., 1979). This rate is probably the limiting step for receptor activation.

We have found that the binding of ATP also rapidly induces changes in the fluorescence properties of the insulin receptor. Specifically, we observe a decrease in intensity, a shift in the emission toward higher energies and an increase in the anisotropy. The anisotropy data show that the greatest change occurs very rapidly within the first minute ($t_{1/2}$ < 1 min) with minor changes thereafter. Two interesting observations stem from the ATP anisotropy data. First, the ATP-dependent increase in anisotropy is doubled in the presence of insulin. Second, in the presence of 160 nM insulin, binding of the non-hydrolyzable ATP analog gave an anisotropy change equivalent to ATP in the absence of insulin. It has been shown that this ATP analog competes with ATP for binding to the receptor (Shia & Pilch, 1983). Since there are two possible ATP binding sites, one per each β subunit, and insulin causes a 2-fold increase in the ATP-dependent change in anisotropy, we postulate that the presence of insulin allows the rapid binding of a second ATP molecule to the receptor (see Figure 5). This can occur only if the ATP molecule can be hydrolyzed or rapidly form a transition state where a labile γ-phosphate is required, since AMP−PNP does not show this effect. This seems to be a plausible explanation of the data, although other interpretations may be possible.

This interpretation is supported by the studies of Baron et al. (1992) who used site-specific antibodies combined with kinase-deficient receptor to show that the latter undergoes an insulin-dependent conformational change despite not binding ATP. They proposed that the same change in the native receptor might allow ATP binding, and we show here that this binding appears to have two parts, one ligand-dependent and the other not. Furthermore, the crystal structure of the soluble insulin receptor kinase domain reveals that the primary site of autophosphorylation, tyrosine 1162, blocks ATP binding (Hubbard et al., 1994). These authors proposed that this would prohibit *cis* autophosphorylation in the basal state and that insulin binding would cause a conformational change in the receptor allowing ATP binding and trans phosphorylation of tyrosine 1162 as the initial event in receptor autophosphorylation and activation. Experimental support for the *trans* phosphorylation model derives from studies of chimeric insulin receptors consisting of one kinase half and one inactive half (Frattali et al., 1992). Indirect support for a *trans*-type mechanism comes from the asymmetry of insulin-dependent receptor autophosphorylation (Lee et al., 1993). Here, we show that initial autophosphorylation event involves only one half of the receptor (Figure 4), and we propose that this occurs *in trans*. However, a surprising result from the experiment of Figure 4 is that, at or before 1 min of phosphorylation, the apparent ratio of phosphorylated $\alpha\beta$ half-receptor to holoreceptor is less than 50%. This is a very consistent result that has at least two possible explanations. The first is that the very low level of autophosphorylation at early times precludes an accurate determination of $\alpha\beta$ receptor amount, and we favor this explanation. Another possibility is that the holoreceptor may exist as a non-covalent dimer, although sedimentation analysis of the receptor in sucrose gradients offers no support for this hypothesis (Böni-Schnetzler et al., 1986).

From these results, we propose a model for receptor activation as shown in Figure 5. Here, insulin (at high concentrations) and ATP bind to the receptor at very fast (diffusion controlled) rates (k_1 and k_2). Insulin binding allows a second molecule of ATP to bind and it also produces a slower conformational change (k_3) which is transmitted throughout the protein. This conformational change then allows for initial autophosphorylation on one half of the molecule followed by full autophosphorylation and kinase activation. Kinetic analysis of the sites of phosphorylation indicate that the tri-tyrosine region, including tyrosine 1162

(see Results) are phosphorylated first followed by tyrosines in other regions of the receptor (White et al., 1984; Tornqvist & Avruch, 1988; Tavaré & Denton, 1988; Lee et al., 1993). It is not clear, however, if a single conformational change governs all autophosphorylation or if multiple steps occur. Once this process begins, it needs about 10 min (at 23−25 °C) to go to completion, and the end result is a 60:40 asymmetry with respect to the site of BBpa-insulin cross-linking (Lee et al., 1993). It is not clear from our own or other studies if any *cis* phosphorylation occurs once autophosphorylation is initiated. This possibility, i.e., a β subunit phosphorylating itself, is indicated in the penultimate receptor model (lower middle, arrow and question mark).

What is the nature of the conformational changes induced by insulin? Based on studies showing that autophosphorylation is asymmetric with respect to the $\alpha\beta$ half-receptors (Lee et al., 1993), and the result that hormone binding brings about a burial of tryptophan residues, we postulate that the effect of insulin is to move the $\alpha\beta$ halves into closer proximity. This idea is supported by studies showing more facile cross-linking of the α subunits in the presence of insulin (Waugh & Pilch, 1989) and, indirectly, by mutational studies of the transmembrane domain of the receptor showing that activation of kinase can occur without stimulation by ligand (Yamada et al., 1992; Cheatham et al., 1993). Experiments pertaining to factors that control the rate of conversion of the hormone-free versus the intrinsically activated state are currently underway.

In conclusion, the reaction scheme depicted in Figure 5 best fits the data acquired by real time fluorescence studies. Other physical techniques must be used to test the validity of this model. The ability to obtain large amounts of recombinant holoreceptor may now allow for these types of studies.

ACKNOWLEDGMENT

We thank Gino Vallega for help with cell culture, Heather McBath for her assistance with the fluorescence studies, and Dr. Walter Zurawsky for his helpful discussions.

REFERENCES

Baron, V., Gautier, N., Komoriya, A., Hainaut, P., Scimeca, J. C., Mervic, M., Lavielle, S., Dolais-Kitabgi, J., & Van Obberghen, E. (1990) *Biochemistry 29*, 4634−4641.

Baron, V., Kaliman, P., Gautier, N., & Van Obberghen, E. (1992) *J. Biol. Chem. 267*, 23290−23294.

Böni-Schnetzler, M., Rubin, J., & Pilch, P. F. (1986) *J. Biol. Chem. 261*, 15281−15287.

Böni-Schnetzler, M., Scott, W., Waugh, S. M., DiBella, E., & Pilch, P. F. (1987) *J. Biol. Chem. 262*, 8395−8401.

Careri, G., Fasell, P., & Gratton, E. (1979) *Annu. Rev. Biophys. Bioeng. 8*, 69−87.

Cheatham, B., Shoelson, S. E., Yamada, K., Goncalves, E., & Kahn, C. R. (1993) *Proc. Natl. Acad. Sci. U.S.A. 90*, 7336−7340.

Christiansen, K., Tranum-Jensen, J., Carlsen, J., & Vinten, J. (1991) *Proc. Natl. Acad. Sci. U.S.A. 88*, 249−252.

Clark, S., & Konstantopoulos, N. (1993) *Biochem. J. 292*, 217−223.

De Meyts, P., Roth, J., Neville, D. M., Jr., Gavin, J. R., III, & Lesniak, M. A. (1973) *Biochem. Biophys. Res. Commun. 55*, 154−161.

Ebina, Y., Ellis, L., Jarnagin, K., Edery, M., Graf, L., Clauser, E., Ou, J. H., Masiarz, F., Kan, Y. W., Goldfine, I. D., Roth, R. A., & Rutter, W. J. (1985) *Cell 40*, 747−758.

Frattali, A. L., Treadway, J. L., & Pessin, J. E. (1992) *J. Biol. Chem. 267*, 19521−19528.

Herrera, R., & Rosen, O. M. (1986) *J. Biol. Chem. 261*, 11980−11985.

Hing, F., Lee, J., Pilch, P. F., & Shipley, G. G. (1993) *Exp. Clin. Endocrinol. 101*, 36−37.

Hubbard, S. R., Wei, L., Ellis, L., & Hendrickson, W. A. (1994) *Nature 372*, 746−754.

Kleinfeld, A. (1988) *Spectroscopic Membrane Probes*, pp 64−92, CRC Press, Inc., Boca Raton, FL.

Kohanski, R. A. (1993) *Biochemistry 32*, 5766−5772.

Laemmli, U. K. (1970) *Nature (London) 227*, 680−685.

Lee, J., & Pilch, P. F. (1994) *Am. J. Physiol. Cell Physiol. 266*, C319−C334.

Lee, J., O'Hare, T., Pilch, P. F., & Shoelson, S. E. (1993) *J. Biol. Chem. 268*, 4092−4098.

Levine, B. A., Clack, B., & Ellis, L. (1991) *J. Biol. Chem. 266*, 3565−3570.

Maddux, B. A., & Goldfine, I. D. (1991) *J. Biol. Chem. 266*, 6731−6736.

Markussen, J., Halstrom, J., Wiberg, F. C., & Schaffer, L. (1991) *J. Biol. Chem. 266*, 18814−18818.

Matayoshi, E., Wang, G., Kraft, G., & Erickson, J. (1990) *Science 247*, 954−958.

Morrison, B., Swanson, M., Sweet, L., & Pessin, J. (1988) *J. Biol. Chem. 263*, 7806−7813.

Nemenoff, R. A., Kwok, Y. C., Shulman, G. I., Blackshear, P. J., Osathanondh, R., & Avruch, J. (1984) *J. Biol. Chem. 259*, 5058−5065.

O'Hare, T., & Pilch, P. F. (1988) *Biochemistry 27*, 5693−5700.

Pang, D. T., & Shafer, J. A. (1983) *J. Biol. Chem. 258*, 2514−2518.

Pang, D. T., & Shafer, J. A. (1984) *J. Biol. Chem. 259*, 8589−8596.

Perlman, R., Bottaro, D. P., White, M. F., & Kahn, C. R. (1989) *J. Biol. Chem. 264*, 8946−8950.

Schaefer, E. M., Siddle, K., & Ellis, L. (1990) *J. Biol. Chem. 265*, 13248−13253.

Schaefer, E. M., Erickson, H. P., Federwisch, M., Wollmer, A., & Ellis, L. (1992) *J. Biol. Chem. 267*, 23393−23402.

Schenker, E., & Kohanski, R. A. (1988) *Biochem. Biophys. Res. Commun. 157*, 140−145.

Schlessinger, J., & Ullrich, A. (1992) *Neuron 9*, 383−391.

Schöffer, L. (1994) *Eur. J. Biochem. 221*, 1127−1132.

Shia, M. A., & Pilch, P. F. (1983) *Biochemistry 22*, 717−721.

Shoelson, S. E., Lee, J., Lynch, C. S., Backer, J. M., & Pilch, P. F. (1993) *J. Biol. Chem. 268*, 4085−4091.

Stephanopoulos, G. (1984) *Chemical Process Control*, pp 186−197, Prentice-Hall, Englewood Cliffs, NJ.

Sweet, L. J., Morrison, B. D., & Pessin, J. E. (1987) *J. Biol. Chem. 262*, 6939−6942.

Tavaré, J. M., & Denton, R. M. (1988) *Biochem. J. 252*, 607−615.

Tavaré, J. M., & Siddle, K. (1993) *Biochim. Biophys. Acta, Mol. Cell Res. 1178*, 21−39.

Taylor, S. I., Cama, A., Accili, D., Barbetti, F., Quon, M. J., De la Luz Sierra, M., Suzuki, Y., Koller, E., Levy-Toledano, R., Wertheimer, E., Moncada, V. Y., Kadowaki, H. & Kadowaki, T. (1992) *Endocr. Rev. 13*, 566−595.

Tornqvist, H. E., & Avruch, J. (1988) *J. Biol. Chem. 263*, 4593−4601.

Towbin, H., Staehelin, T., & Gordon, J. (1979) *Proc. Natl. Acad. Sci. U.S.A. 76*, 4350−4354.

Ullrich, A., Bell, J. R., Chen, E. Y., Herrera, R., Petruzzelli, L. M., Dull, T. J., Gray, A., Coussens, L., Liao, Y. C., Tsubokawa, M., Mason, A., Seeburg, P. H., Grunfeld, C., Rosen, O. M., & Ramachandran, J. (1985) *Nature (London) 313*, 756−761.

Wang, S., Martin, E., Cimino, J., Omann, G., & Glaser, M. (1988) *Biochemistry 27*, 2033−2039.

Waugh, S. M., & Pilch, P. F. (1989) *Biochemistry 28*, 2722−2727.

White, M. F., Haring, H. U., Kasuga, M., & Kahn, C. R. (1984) *J. Biol. Chem. 259*, 255−264.

Yamada, K., Goncalves, E., Kahn, C. R., & Shoelson, S. E. (1992) *J. Biol. Chem. 267*, 12452−12461.

BI961815G